

Unbalanced Response and Design Optimization of Rotor by ANSYS and Design Of Experiments

Ritesh Fegade^a, Vimal Patel^b

Abstract

In this paper harmonic analysis of rotor is done to identify the frequency through variation in the diameters by design of optimization (DOE) and ANSYS parametric design. In DOE two levels were used with total eleven diameters as parameters, which resulted in forty eight runs as per Plakett-Burman design to obtain responses using ANSYS. The effect graphs were studied to identify the diameters which are responsible for producing major effects on the frequency. It was seen that diameters D10 and D12 producing major effects, which were then used to identify the critical frequency of rotor.

Key words: ANSYS Parametric Design, Design of optimization, harmonic analysis, rotor, DOE, Unbalance Response etc.

1. Introduction

DOE is a systematic approach to investigation of a system or process. A series of structured tests are designed in which planned changes are made to the input variables of a process or system. The effects of these changes on a pre-defined output are then assessed.

Design of Experiments (DOE) techniques enables designers to determine simultaneously the individual and interactive effects of many factors that could affect the output results in any design. DOE also provides a full insight of interaction between design elements; therefore, it helps turn any standard design into a robust one. Simply put, DOE helps to pin point the sensitive parts and sensitive areas in designs that cause problems in Yield. Designers are then able to fix these problems and produce robust and higher yield designs prior going into production.

Vibration control of turbo machinery is very important for the integrity of industrial plants. In this regard it is very important to predict the dynamic behavior of rotating machinery which operates above the first critical speed accurately. In fact, rotating motion and critical speeds are design criteria of rotating machinery and play an important role in diagnosis and control of rotors.

Harmonic response analysis is a technique used to determine the steady-state response of a linear structure to loads that vary sinusoidally (harmonically) with time and is used to predict the sustained dynamic behavior of structures to consistent cyclic loading. Thus, it can be verified whether or not a machine design will successfully overcome resonance, fatigue, and other harmful effects of forced vibrations.

ANSYS is a common tool for finite element analyses and it is widely used in research and development of rotating machinery. It has rotating beam elements such as BEAM188, BEAM4 element and PIPE16 elements which can be used to model the shaft. For a rotating beam element, the gyroscopic effect can be taken into consideration. Also, the effects of rotary inertia, shear deformation, axial load and internal damping can be included. However, this paper like most others doesn't set specific elements for modeling rotating disks and bearings. This paper shows how MATRIX27 element is used to model rotating disks and bearing. The geometry of this arbitrary element is undefined, but its mechanism can be specified by stiffness, damping or mass matrix. Specifications for the elements, descriptions and the critical speed calculations of rotor-bearing system are included in this paper.

The use of flexible supports was strongly developed during last few years due to some practical advantages offered by this design. A number of authors [1,6,7,8,11,12,13,18,21,22,23] have addressed the problem, highlighted the importance of this

component, and tried to use experimental procedures and data in order to undertake the influence of the support flexibility of rotor machinery. Effectively, the dynamic behavior of rotating machines may be drastically affected by the characteristics of the support flexibility of rotor machinery. Then, one of the main objectives of the researchers and designers was to be able to obtain fundamental mathematical models, adequate to the observed physical phenomena, in order to predict numerically the dynamic behavior of rotor systems and the influence of the support flexibility of rotors. In recent year there has been an important research activity in the field of modeling and analysis of the dynamic behavior of rotating machinery in order to adjust some system parameters and to obtain the most suitable design within the speed range of interest. Then, the utilization of finite element models in the area of rotor dynamics was applied to develop suitable models and has yielded highly successful results [1, 11]. These numerical models are now used to design machinery to operate within acceptable limits.

Taplak[9] in his paper studied a program named Dynrot was used to make dynamic analysis and the evaluation of the results. For this purpose, a gas turbine rotor with certain geometrical and mechanical properties was modeled and its dynamic analysis was made by Dynrot program. Gurudatta[4] in his paper presented an alternative procedure called harmonic analysis to identify frequency of a system through amplitude and phase angle plots. The unbalance that exists in any rotor due to eccentricity has been used as excitation to perform such an analysis. ANSYS parametric design language has been implemented to achieve the results

Sinou[17] investigated the response of a rotor's non-linear dynamics which is supported by roller bearings. He studies on a system comprised of a disk with a single shaft, two flexible bearing supports and a roller bearing. He found that the reason of the exciter is imbalance. He used a numerical method named Harmonic Balance Method for this study. Chouskey[14] et.al studied the influences of internal rotor material damping and the fluid film forces (generated as a result of hydrodynamic action in journal bearings) on the modal behavior of a flexible rotor-shaft system. It is seen that correct estimation of internal friction, in general, and the journal bearing coefficients at the rotor spin-speed are essential to accurately predict the rotor dynamic behaviour. This serves as a first step to get an idea about dynamic rotor stress and, as a result, a dynamic design of rotors.

Whalley and Abdul-Ameer[19], calculated the rotor resonance, critical speed and rotational frequency of a shaft that its diameter changes by the length, by using basic harmonic response method. Gasch[16], investigated the dynamic behavior of a Laval (Jeffcott) rotor with a transverse crack on its elastic shaft, and developed the non-linear motion equations which gave important clues on the crack diagnosis.

Das et al [2] aimed to develop an active vibration control scheme to control the transverse vibrations on the rotor shaft arising from imbalance and they performed an analysis on the vibration control and stability of a rotor- shaft system which has electromagnetic exciters.

Villa et al [5] studied the non-linear dynamic analysis of a flexible imbalanced rotor supported by roller bearings. They used Harmonic Balance Method for this purpose. Stability of the system was analyzed in frequency term with a method based on complexity. They showed that Harmonic Balance Method has realized the AFT strategy and harmonic solution very efficiently. Lei and Palazzolo[20] have analyzed a flexible rotor system supported by active magnetic bearings and synthesized the Campbell diagrams, case forms and eigen values to optimize the rotor-dynamic characteristics and obtained the stability at the speed range. They also investigated the rotor critical speed, case forms, frequency responses and time responses.

Considering literature review there seems to be a literature gap of not using DOE for rotor balancing. As seen from literature this paper is first attempt which uses DOE as well as ANSYS parametric design for optimization of rotor. In this paper harmonic analysis of rotor is done to identify the excitation frequency through variation in the diameters by design of optimization (DOE) and ANSYS parametric design. In DOE two levels were used with total eleven diameters as parameters, which resulted in forty eight combinations to obtain responses using ANSYS. The effect graphs were seen to identify the diameters which are responsible for producing major effects on the frequency. It was seen that diameters D10 and D12

producing major effects, which were then used to identify the critical frequency of rotor. In this paper first the methodology is explained followed by results and discussion, and conclusion.

2. Methodology

The Nelson rotor is selected here for optimization. In DOE two levels are used with eleven parameters which resulted in forty eight combinations. Responses of forty eight combinations are obtained by ANSYS. Effects of these diameters on frequency are observed in DOE. MINITAB 15 is used for this purpose.

2.1 Model

The model considered is a Nelson rotor [15] which is a 0.355(m) long overhanging steel shaft of 14 different cross sections. The shaft carries a rotor of mass 1.401(kg) and eccentricity 0.635(cm) at 0.0889(m) from left end and is supported by firstly two bearings at a distance of 0.1651(m) and 0.287(m) from the left end respectively. Six stations are considered during harmonic analysis as shown in Fig.7, where station numbers denote different nodes in the model (1) Left extreme of shaft, (2) Disc, (3) First bearing node, (4) Between the two bearings, (5) Second bearing node and (6) Right extreme of shaft.

A density of 7806 kg/m^3 and elastic modulus $2.078\text{E}11 \text{ n/m}^2$ were used for the distributed rotor and a concentrated disk with a mass of 1.401 kg, polar inertia 0.002 kg.m^2 and diametral inertia 0.00136 kg.m^2 was located at station five. Fluid film bearing was used for analysis.

2.2 Geometric Modeling and Finite Element Modeling Using APDL

In critical speed calculations of rotor-bearing systems, BEAM188 and MATRIX27 elements are adopted.

2.2.1 Beam188

The multisection shaft has been modeled in ANSYS using Beam 188 which is a linear/quadratic two node beam element in three dimensions with six degrees of freedom at each node: translations in the nodal x, y and z directions and rotations about nodal x, y and z axes. This element facilitates the meticulous definition of all the cross sections of the shaft. The rotor and its real constants include: AREA, SPIN, ADDMAS. SPIN is an important item in the critical speed calculations, which defines the rotational speed of the shaft. ADDMAS defines added masses along the shaft. The nodes, elements, material properties, real constants, boundary conditions and other physical system defining features that constitute the model have been created by exclusively using APDL commands such as ET, MAT, K, N, LSTR, R, RMORE, LATT, LESIZE and E.

2.2.2 Mass21

The disk of the rotor has been modeled using element MASS21. Its Real Constants include: IZZ, IYY, IXX.

2.2.3 Matrix27

The fluid film bearing has been modeled in ANSYS using MATRIX27. It represents an arbitrary element whose geometry is undefined but whose mechanism can be specified by stiffness, damping, or mass matrix coefficients. The matrix is assumed to relate two nodes, each with six degrees of freedom per node: translations in the nodal x, y and z directions and rotations about the nodal x, y and z axes. There are three options to use the MATRIX27 to define coefficients, which is very useful to model linear cross coupling bearing characteristics and gyroscopic damping matrix for rotating disks.

2.3 Design of Experiment

Table 1 shows 48 runs required for two levels factorial design and eleven parameters as per Plakett-Burman design in DOE. The parameter used here are all diameters of the Nelson rotor. A response that is excitation frequency is obtained for each with help of ANSYS software. DOE is performed to found out the effect of each diameter on frequency.

Table 1 Runs used in DOE

	D1	D2	D3	D4	D6	D8	D10	D12	D14	D16	D17	FRQ
1	0.0152	0.0154	0.0102	0.0356	0.071	0.0458	0.0304	0.0354	0.0204	0.0712	0.0356	293.33
2	0.0052	0.0254	0.0102	0.0456	0.071	0.0458	0.0304	0.0254	0.0304	0.0712	0.0456	253.33
3	0.0052	0.0154	0.0102	0.0356	0.061	0.0458	0.0204	0.0254	0.0304	0.0812	0.0456	213.33
4	0.0052	0.0254	0.0102	0.0456	0.071	0.0458	0.0304	0.0254	0.0304	0.0712	0.0456	253.33
5	0.0152	0.0254	0.0102	0.0356	0.061	0.0558	0.0304	0.0254	0.0304	0.0812	0.0356	266.67
6	0.0152	0.0254	0.0204	0.0456	0.071	0.0558	0.0304	0.0354	0.0304	0.0812	0.0456	266.67
7	0.0052	0.0254	0.0204	0.0356	0.061	0.0458	0.0304	0.0354	0.0304	0.0712	0.0356	293.33
8	0.0152	0.0154	0.0204	0.0356	0.061	0.0558	0.0204	0.0354	0.0304	0.0712	0.0456	213.33
9	0.0052	0.0154	0.0102	0.0356	0.061	0.0458	0.0204	0.0254	0.0304	0.0812	0.0456	213.33
10	0.0152	0.0254	0.0102	0.0456	0.061	0.0458	0.0204	0.0354	0.0204	0.0812	0.0356	200.00
11	0.0152	0.0154	0.0204	0.0456	0.061	0.0458	0.0304	0.0254	0.0204	0.0712	0.0456	266.67
12	0.0052	0.0254	0.0102	0.0356	0.071	0.0558	0.0204	0.0354	0.0204	0.0712	0.0456	200.00
13	0.0152	0.0154	0.0102	0.0456	0.071	0.0558	0.0204	0.0254	0.0304	0.0712	0.0356	200.00
14	0.0152	0.0154	0.0204	0.0356	0.061	0.0558	0.0204	0.0354	0.0304	0.0712	0.0456	213.33
15	0.0152	0.0154	0.0204	0.0456	0.061	0.0458	0.0304	0.0254	0.0204	0.0712	0.0456	266.67
16	0.0052	0.0254	0.0102	0.0456	0.071	0.0458	0.0304	0.0254	0.0304	0.0712	0.0456	253.33
17	0.0152	0.0154	0.0102	0.0456	0.071	0.0558	0.0204	0.0254	0.0304	0.0712	0.0356	200.00
18	0.0052	0.0254	0.0204	0.0356	0.061	0.0458	0.0304	0.0354	0.0304	0.0712	0.0356	293.33
19	0.0052	0.0254	0.0204	0.0456	0.061	0.0558	0.0204	0.0254	0.0204	0.0712	0.0356	186.67
20	0.0152	0.0154	0.0204	0.0356	0.061	0.0558	0.0204	0.0354	0.0304	0.0712	0.0456	213.33
21	0.0052	0.0154	0.0102	0.0456	0.061	0.0558	0.0304	0.0354	0.0204	0.0812	0.0456	293.33
22	0.0052	0.0254	0.0102	0.0356	0.071	0.0558	0.0204	0.0354	0.0204	0.0712	0.0456	200.00
23	0.0052	0.0154	0.0102	0.0356	0.061	0.0458	0.0204	0.0254	0.0304	0.0812	0.0456	213.33
24	0.0152	0.0254	0.0204	0.0456	0.071	0.0558	0.0304	0.0354	0.0304	0.0812	0.0456	266.67
25	0.0052	0.0154	0.0102	0.0456	0.061	0.0558	0.0304	0.0354	0.0204	0.0812	0.0456	293.33
26	0.0152	0.0254	0.0102	0.0456	0.061	0.0458	0.0204	0.0354	0.0204	0.0812	0.0356	200.00
27	0.0052	0.0154	0.0204	0.0456	0.071	0.0458	0.0204	0.0354	0.0304	0.0812	0.0356	213.33
28	0.0052	0.0154	0.0204	0.0356	0.071	0.0558	0.0304	0.0254	0.0204	0.0812	0.0356	266.67
29	0.0052	0.0154	0.0102	0.0456	0.061	0.0558	0.0304	0.0354	0.0204	0.0812	0.0456	293.33
30	0.0152	0.0154	0.0102	0.0456	0.071	0.0558	0.0204	0.0254	0.0304	0.0712	0.0356	200.00
31	0.0052	0.0154	0.0204	0.0456	0.071	0.0458	0.0204	0.0354	0.0304	0.0812	0.0356	213.33
32	0.0152	0.0154	0.0204	0.0456	0.061	0.0458	0.0304	0.0254	0.0204	0.0712	0.0456	266.67
33	0.0152	0.0254	0.0102	0.0356	0.061	0.0558	0.0304	0.0254	0.0304	0.0812	0.0356	266.67
34	0.0052	0.0154	0.0204	0.0456	0.071	0.0458	0.0204	0.0354	0.0304	0.0812	0.0356	213.33
35	0.0152	0.0254	0.0102	0.0356	0.061	0.0558	0.0304	0.0254	0.0304	0.0812	0.0356	266.67
36	0.0152	0.0254	0.0204	0.0356	0.071	0.0458	0.0204	0.0254	0.0204	0.0812	0.0456	200.00
37	0.0152	0.0254	0.0204	0.0356	0.071	0.0458	0.0204	0.0254	0.0204	0.0812	0.0456	200.00
38	0.0152	0.0254	0.0204	0.0356	0.071	0.0458	0.0204	0.0254	0.0204	0.0812	0.0456	200.00
39	0.0152	0.0154	0.0102	0.0356	0.071	0.0458	0.0304	0.0354	0.0204	0.0712	0.0356	293.33

40	0.0152	0.0154	0.0102	0.0356	0.071	0.0458	0.0304	0.0354	0.0204	0.0712	0.0356	293.33
41	0.0052	0.0254	0.0204	0.0356	0.061	0.0458	0.0304	0.0354	0.0304	0.0712	0.0356	293.33
42	0.0052	0.0154	0.0204	0.0356	0.071	0.0558	0.0304	0.0254	0.0204	0.0812	0.0356	266.67
43	0.0052	0.0254	0.0102	0.0356	0.071	0.0558	0.0204	0.0354	0.0204	0.0712	0.0456	200.00
44	0.0152	0.0254	0.0102	0.0456	0.061	0.0458	0.0204	0.0354	0.0204	0.0812	0.0356	200.00
45	0.0052	0.0254	0.0204	0.0456	0.061	0.0558	0.0204	0.0254	0.0204	0.0712	0.0356	186.33
46	0.0052	0.0154	0.0204	0.0356	0.071	0.0558	0.0304	0.0254	0.0204	0.0812	0.0356	266.67
47	0.0052	0.0254	0.0204	0.0456	0.061	0.0558	0.0204	0.0254	0.0204	0.0712	0.0356	186.33
48	0.0152	0.0254	0.0204	0.0456	0.071	0.0558	0.0304	0.0354	0.0304	0.0812	0.0456	266.67

3. ANSYS Solution

Once the finite element model has been prepared, harmonic analysis is performed by applying an unbalance force at the rotor (assuming an eccentricity of 0.635(cm)). The system is solved using frontal solver to find response of the system in terms of amplitude and phase angle plots. Response is determined at six stations (1) Left extreme of shaft, (2)Disc, (3)First bearing node, (4) Between the two bearings, (5) Second bearing node and (6) Right extreme of shaft. The resulting graphs are exported as jpeg files.

In general, any rotating critical speed is associated with high vibration amplitude. When the rotating speed is close to or away from a critical speed, vibration amplitude increases or decreases abruptly and phase becomes unsteady as figure. 8 shows. For rotating machinery, rotor unbalance mass is a kind of synchronous excitation, and induces vibration.

The Harmonic Response Analysis module of ANSYS is applied to calculate unbalance synchronous response of the rotor-bearing system, and a Bode plot can be obtained. From the Bode plot, rotating speeds with peak vibration are defined as critical speeds.

4. Results and Discussion

4.1 Fluid film bearings

The shaft is supported by two fluid film bearings of stiffness component the bearings are $k_{xx} = k_{yy} = 4.378E7$ N/m. while damping components are $C_{zz}=C_{yy}=1752$ (Ns/m). The unbalance response for a disk mass center eccentricity of 0.635(cm) at station two was determined for speed range 4800-28800 rpm. We therefore present the results that correspond to 268.9Hz, which is the first critical speed of the system as calculated by B. Gurudatt, and Vikram Krishna [3]. Fig. 8 through 13 displays the variation of amplitude of vibration of the system at the six identified stations respectively for optimization condition. The maximum value of amplitude obtained was $0.5572E-7$. It can be observed that the amplitude reaches a maximum value at one particular excitation frequency. Fig. 14 displays the typical variation of phase angle with excitation frequency at all the stations for optimization condition.

4.2 Results of DOE

Normal plot of the standardized effect, Parreto chart of the standardized effect, Main effects plot for frequency and Interaction plots of FRE are as shown in figures 1, 2, 3 and 4 respectively.

The Session window output and the two effects plots are as shown below and are used to determine which effects are important to your process. First, look at the Session window output.

Factorial Fit: frequency versus D1, D2, ...

Table 2 Estimated Effects and Coefficients for frequency (coded units)

Term	Effect	Coef	SECoef	T	P
constant		239.152	0.007083	33762.65	0.0
D1	-1.637	-0.818	0.007083	-115.53	0.0
D2	-11.693	-5.847	0.007083	-825.41	0.0
D3	-1.693	-0.847	0.007083	-119.53	0.0
D4	-8.361	-4.180	0.007083	-590.18	0.0
D6	-4.972	-2.486	0.007083	-350.94	0.0
D8	-5.026	-2.513	0.007083	-354.76	0.0
D10	71.696	35.848	0.007083	5060.88	0.0
D12	15.026	7.513	0.007083	1060.65	0.0
D14	1.693	0.847	0.007083	119.53	0.0
D16	1.969	0.848	0.007083	119.71	0.0
D17	-1.639	-0.820	0.007083	-115.71	0.0
D1*D4	-1.637	-0.818	0.007083	-115.53	0.0
D1*D6	8.304	4.152	0.007083	586.18	0.0
D1*D10	-1.693	0.847	0.007083	-119.53	0.0
D1*D12	-5.028	-2.514	0.007083	-354.94	0.0

S = 0.0490748 PRESS = 0.1734

R-Sq = 100.00% R-Sq (pred) = 100.00% R-Sq (adj) = 100.00%

Table 3 Analysis of Variance for frequency (coded units)

Source	DF	Seq SS	Adj SS	Adj MS	F	P
Main	11	67639.9	67639.9	6149.08	2553251.99	0.0

Effects						
2-Way Interactions	4	1197.5	1197.5	299.37	124305.10	0.0
Residual Error	32	0.1	0.1	0.00		
Pure Error	32	0.1	0.1	0.00		
Total	47	68837.5				

Table 4 Unusual Observations for frequency

Obs	Std Order	frequency	Fit	SE Fit	Residual	St Resid
19	15	186.670	186.443	0.028	0.227	5.66R
45	31	186.330	186.443	0.028	-0.113	-2.83R
47	47	186.330	186.443	0.028	-0.113	-2.83R

R denotes an observation with a large standardized residual.

Table 5 Estimated Coefficients for frequency using data in uncoded units

Term	Coef
Constant	179.445
D1	-5878.75
D2	-1169.33
D3	-166.013
D4	-502.203
D6	-2191.22
D8	-502.583
D10	7515.02
D12	2528.36
D14	169.333
D16	169.583

D17	-163.917
D1*D4	-32733.3
D1*D6	166083
D1*D10	-33866.7
D1*D12	-100567

The full fit model, which includes the two main effects and the two-way interaction. We used the p-values (P) in the Estimated Effects and Coefficients table to determine which effects are significant. Using $\alpha = 0.05$, the main effects for diameters D1 to D17 and their interactions are statistically significant; that is, their p-values are less than 0.05.

Next, evaluate the normal probability plot and the Pareto chart of the standardized effects to see which effects influence the response, excitation frequency.

Significant terms are identified by a square symbol. Diameters D10 and D12 and their interactions are significant ($\alpha=0.05$).

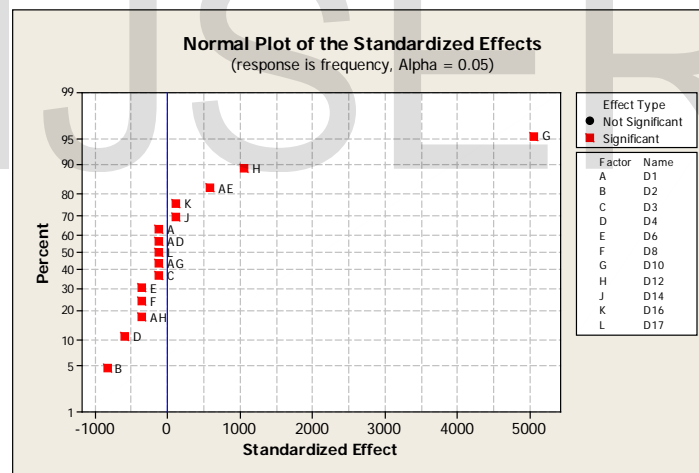


Figure.1. normal plot of the standardized effect

Minitab displays the absolute value of the effects on the Pareto chart as shown in figure 2. Any effects that extend beyond the reference line are significant at the default level of 0.05. Diameters D10 and D12 and their interactions are all significant ($\alpha = 0.05$).

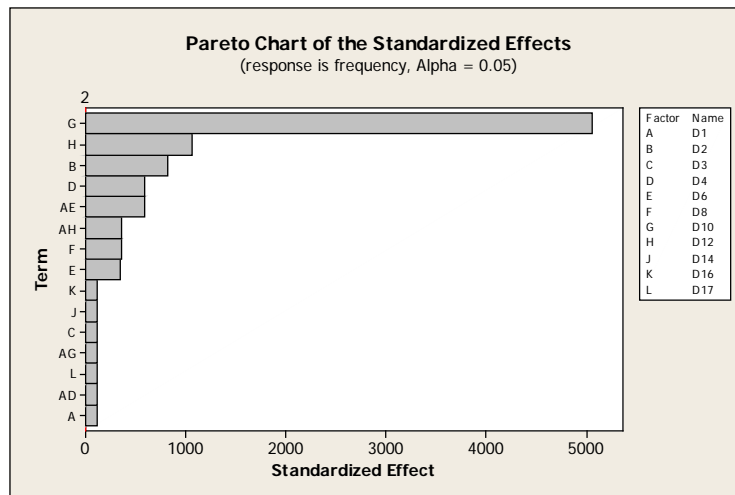


Figure.2. Pareto chart of the standardized effect

Next, the main effect plots are drawn in MINITAB as shown in figure 3. The effect of different diameters on excitation frequency shows, diameters D10 and D12 both increases excitation frequency. The plot also indicates that:

- The diameter D10 has more effect on frequency as compared to D12
- Other diameters are not affecting excitation frequency to much extent.

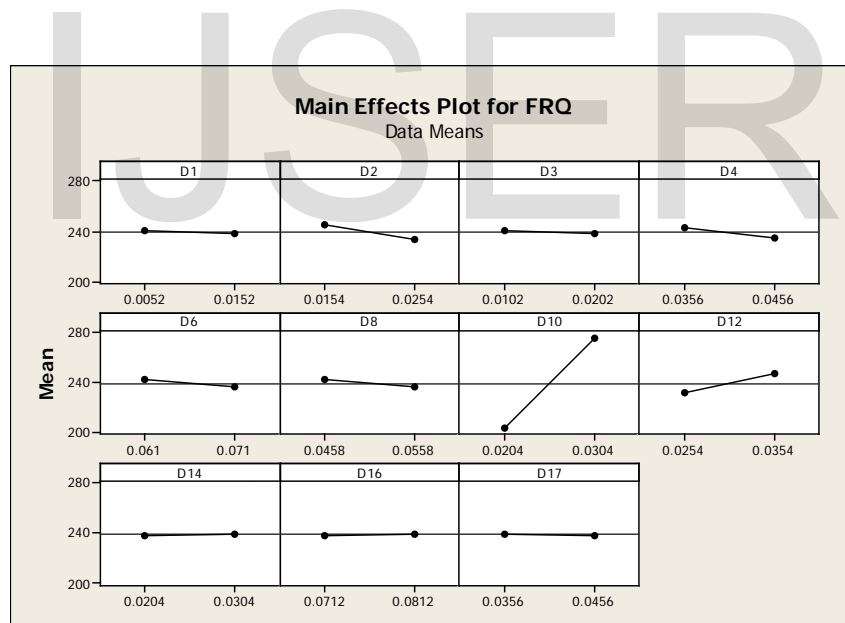


Figure.3. Main effects plot for frequency

An interaction plot figure 4 shows the impact that changing the settings of one factor has on another factor. Because an interaction can magnify or diminish main effects, evaluating interactions is extremely important. Parallel lines in an interaction plot indicate no interaction. The greater the difference in slope between the lines, the higher the degree of interaction. However, the interaction plot doesn't tell you if the interaction is statistically significant.

The plot shows that interaction of D2 and D14 has greater difference in slope between lines. So we can conclude that as D2 values vary from 0.0154 to 0.0254 the frequency reduces, while as D14 values increases from 0.0204 to 0.0304 the frequency

increases. Similarly D4 and D17 interaction shows the similar effect that is as D4 values increases frequency decreases and as D17 value increases frequency increases. Similarly D8 and D16 shows same kind of interaction as D8 values increases frequency decreases and as D17 value increases frequency increases.

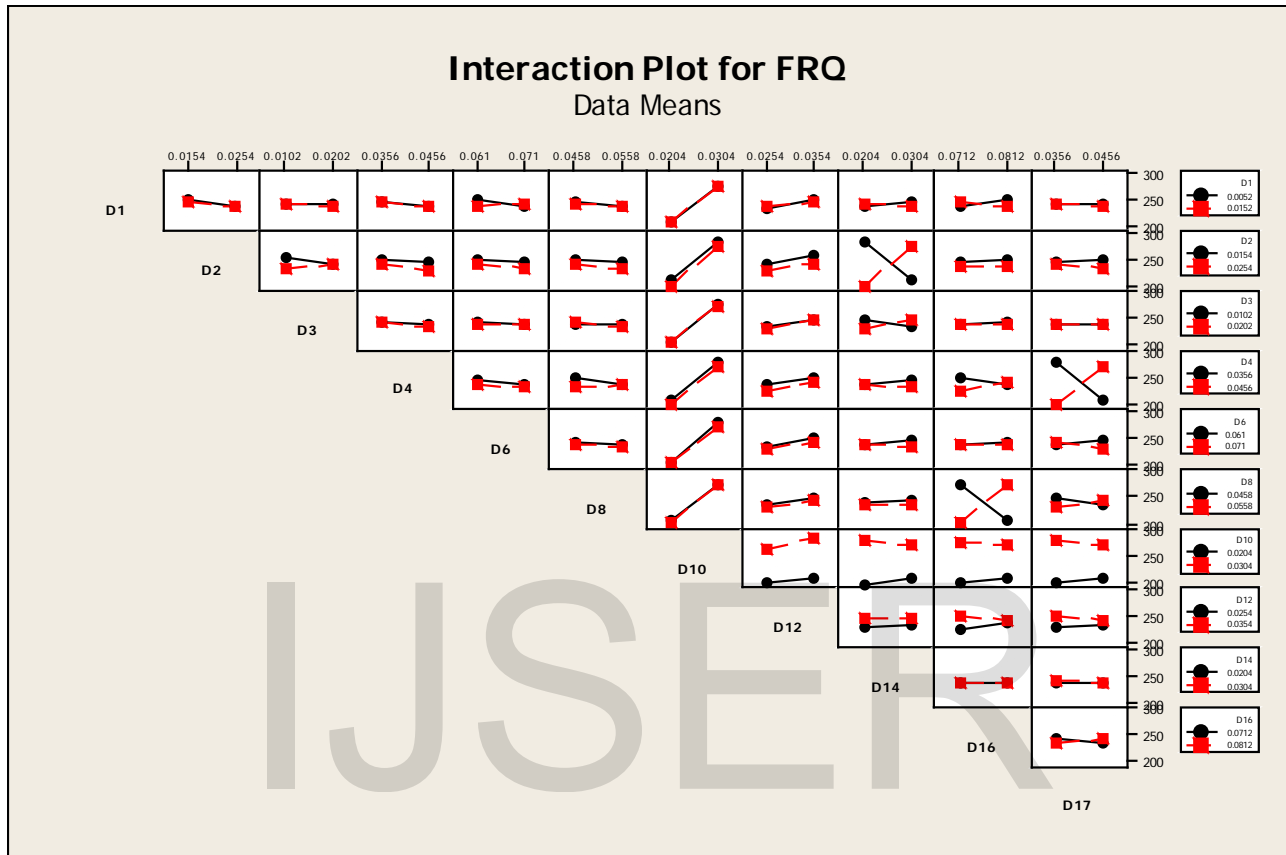


Figure.4 Interaction plot for frequency

4.3 Optimization chart

After determining D10 and D12 as the main diameter affecting excitation frequency, the optimization charts are drawn based on values of frequencies obtained from ANSYS software. The figure 5 shows the graph of excitation frequencies obtained for different diameters. The critical value of excitation frequency 306.67 Hz is obtained at 2.02×10^{-2} meter. Similar figure 6 shows the graph of excitation frequencies obtained from different diameters. The critical value of excitation frequency 266.67 Hz is obtained at 1.77×10^{-2} meter.

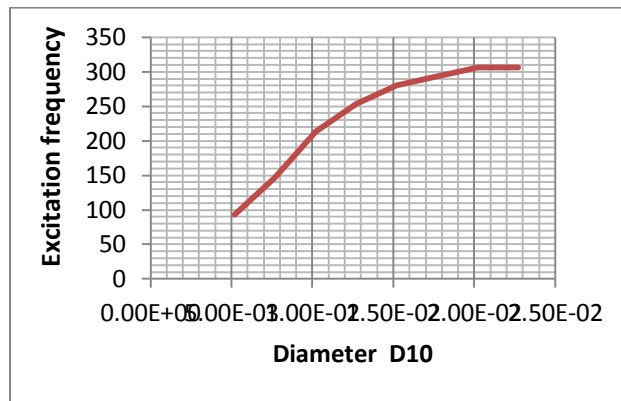


Figure.5 Graph for excitation frequency Vs diameter D10

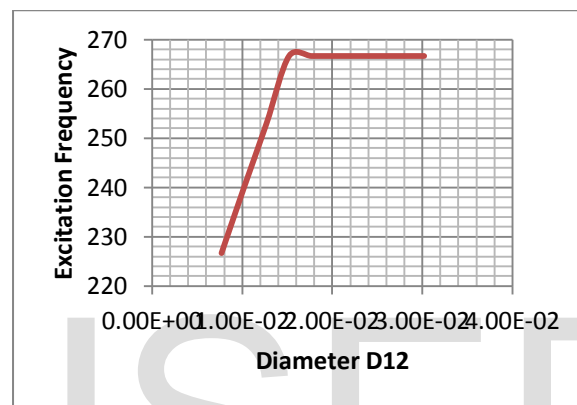


Figure 6 Graph for excitation frequency Vs diameter D12

5. Conclusion

A finite element model of multi-bearing rotor system using ANSYS is presented in this paper. The effects of rotary inertia, and internal damping were included in the analysis. The attempt has been made to optimize the design that is maximizing excitation frequency by changes in diameters. The systematic design of experimentation ANSYS parametric design is used for this purpose. The results shows diameter D10 and D12 has major effect on excitation frequency for the fluid film bearing selected maximum excitation frequency is obtain 306.67 for D10 and maximum excitation frequency 266.67 for D12.

The study has certain limitation. In this study only effect of changing diameters on excitation frequency is seen and optimization is done. The other dimensional effects, material of shaft, and other type of bearings can be studied in future for rotor balancing.

Table.6 Geometric Data of Rotor-Bearing Element

Element Node No	Node Location (cm)	Bearing and Disk	Inner Diameter (cm)	Outer Diameter (cm)
1	0.0		0.0	0.51
2	1.27		0.0	1.02
3	5.08		0.0	0.76
4	7.62		0.0	2.03
5	8.89	Disk	0.0	2.03

6	10.16		0.0	3.30
7	10.67		1.52	3.30
8	11.43		1.78	2.54
9	12.70		0.0	2.54
10	13.46		0.0	1.27
11	16.51	Bearing	0.0	1.27
12	19.05		0.0	1.52
13	22.86		0.0	1.52
14	26.67		0.0	1.27
15	28.70	Bearing	0.0	1.27
16	30.48		0.0	3.81
17	31.50		0.0	2.03
18	34.54		1.52	2.03

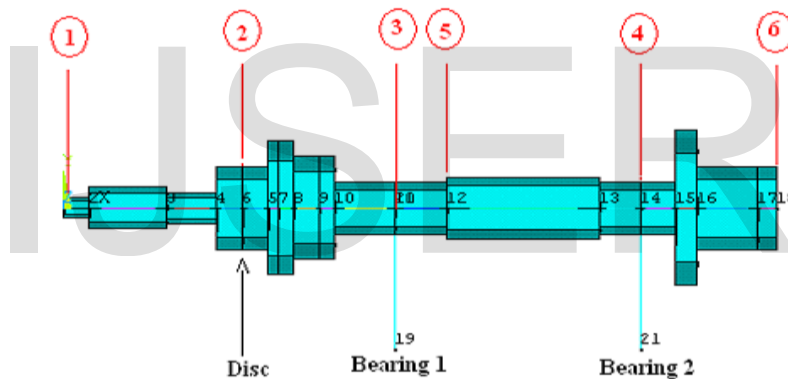


Figure 7: Model of Nelson rotor with various sections, disc and bearings.
 Numbers in red indicate station numbers

References

1. A. W. Lees and M. I. Friswell, (1997) "The Evaluation of Rotor Imbalance in Flexibly Mounted Machines", Journal of Sound and Vibration", vol. 208, no. 5, pp. 671–683.
2. A.S. Das, M.C. Nighil, J.K. Dutt, H. Irretier, (2008) "Vibration Control and Stability Analysis of Rotor-Shaft System with Electromagnetic Exciters", Mechanism and Machine Theory 43 (10), pp.1295–1316.
3. ANSYS 11.0 help document.
4. B. Gurudatt, S. Seetharamu, P. S. Sampathkumaran and Vikram Krishna, (2010) "Implementation, of Ansys Parametric Design Language for the Determination of Critical Speeds of a Fluid Film Bearing Supported Multi Sectioned Rotor with Residual Unbalance Through Modal and Out Of Balance Response Analysis", Proceedings of the World Congress on Engineering Vol II.
5. C. Villa, J.J. Sinou, F. Thouverez, (2008) "Stability and Vibration Analysis of A Complex Flexible Rotor Bearing System", Communications in Nonlinear Science and Numerical Simulation 13 (4), pp.804–821.

6. D. Childs John Wiley & Sons, (1993) "Turbomachinery Rotordynamics: Phenomena, Modeling, and Analysis", New York, NY, USA,
7. D.E.Bently, C.T.Hatch, and B. Grissom, (2002) "Fundamentals of Rotating Machinery Diagnostics, Bently Pressurized Bearing Press", Minden, Nev, USA.
8. F. F. Ehrich, Ed, (1992) "Handbook of Rotordynamics", McGraw-Hill, New York, NY, USA.
9. Hamdi Taplak, Mehmet Parlak, (2012) "Evaluation of Gas Turbine Rotor Dynamic Analysis Using the Finite Element Method", Measurement 45 pp.1089–1097.
10. Howard J. Seltman (2012) "Experimental Design and Analysis", January 30.
11. J. A. V'azquez, L. E. Barrett, and R. D. Flack, (2001) "A Flexible Rotor on Flexible Bearing Supports: Stability and Unbalance Response", Journal of Vibration and Acoustics, vol. 123, no. 2, pp.137–144.
12. J. K. Dutt and B. C.Nakra, (1995) "Dynamics of Rotor Shaft System on Flexible Supports With Gyroscopic Effects", Mechanics Research Communications, vol. 22, no. 6, pp. 541–545.
13. J. M. Vance, (1988) "Rotordynamics of Turbomachinery", John Wiley & Sons, New York, NY, USA.
14. M. Chouksey, J.K. Dutt, S.V. Modak, (2012) "Modal Analysis of Rotor-Shaft System Under The Influence of Rotor-Shaft Material Damping and Fluid Film Forces", Mechanism and Machine Theory 48 pp.81–93.
15. Nelson, H.D. et al (1976) "The Dynamics of Rotor Bearing System Using Finite Elements", ASME Journal of Engineering For Industry Vol.98, No.2, pp.593-600.
16. R. Gasch, (2008) "Dynamic Behaviour of the Laval Rotor with A Transverse Crack", Mechanical Systems and Signal Processing 22 (4) pp.790–804.
17. R. Sinou, T.N. Baranger, E. Chatelet, G. Jacquet, (2008) "Dynamic Analysis of A Rotating Composite Shaft", Composites Science and Technology 68 (2) pp.337–345.
18. R. Tiwari and N. S. Vyas, (1997) "Non-linear Bearing Stiffness Parameter Extraction From Random Response in Flexible Rotor Bearing Systems", Journal of Sound and Vibration, vol. 203, no. 3, pp. 389–408.
19. R. Whalley, A. Abdul-Ameer, (2009) "Contoured Shaft and Rotor Dynamics", Mechanism and Machine Theory 44 (4) pp.772–783.
20. S. Lei, A. Palazzolo, (2008) "Control of Flexible Rotor Systems with Active Magnetic Bearings", Journal of Sound and Vibration 314 (1–2) pp.19–38.
21. S. Okamoto, M. Sakata, K. Kimura, and H. Ohnabe, (1995) "Vibration Analysis of a High Speed and Light Weight Rotor System Subjected to a Pitching or Turning Motion II: A Flexible Rotor System on Flexible Suspensions", Journal of Sound and Vibration, vol. 184, no. 5, pp. 887–906.
22. S.E dwards, A.W. Lees and M.I. Friswell, (2000) "Experimental Identification of Excitation and Support Parameters of A Flexible Rotor Bearings Foundation System from A Single Run Down", Journal of Sound and Vibration, vol. 232, no. 5, pp. 963–992.

Optimization plots for fluid film bearings

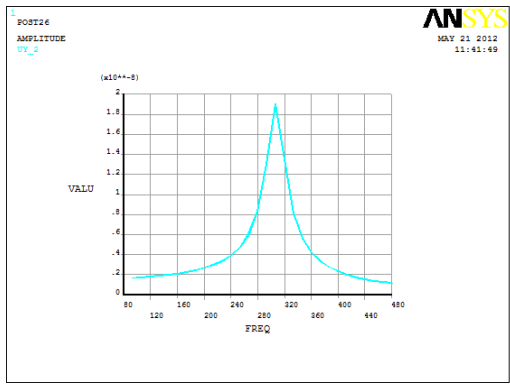


Figure 8: Variation of amplitude of vibration (m)(on Y axis) at station 1 with excitation frequency (Hz)(on X axis)

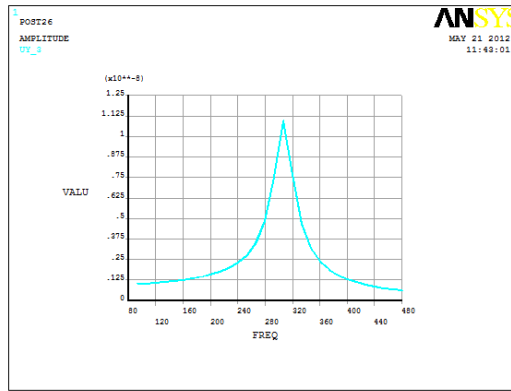


Figure 9: Variation of amplitude of vibration (m)(on Y axis) at station 2 with excitation frequency (Hz)(on X axis)

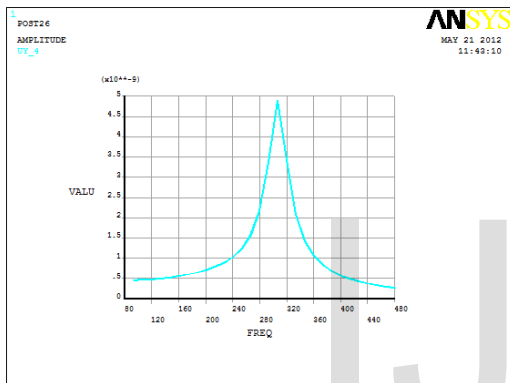


Figure 10: Variation of amplitude of vibration (m)(on Y axis) at station 3 with excitation frequency (Hz)(on X axis)

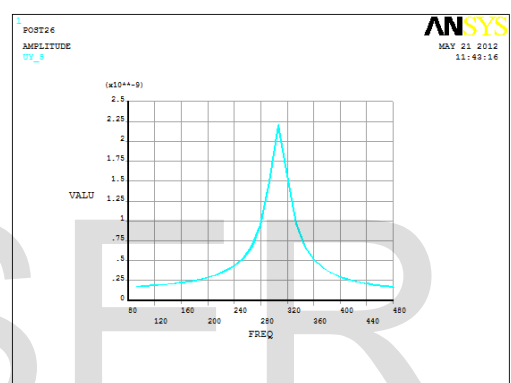


Figure 11: Variation of amplitude of vibration (m)(on Y axis) at station 4 with excitation frequency (Hz)(on X axis)

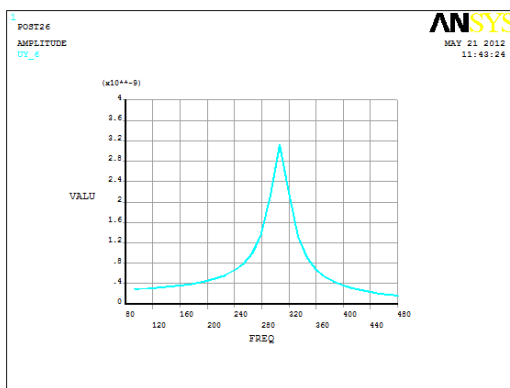


Figure 12: Variation of amplitude of vibration (m)(on Y axis) at station 5 with excitation frequency (Hz)(on X axis)

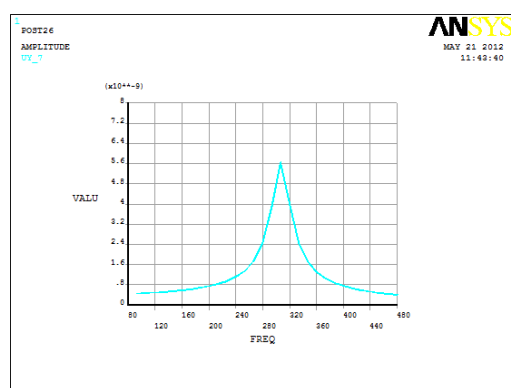


Figure 13: Variation of amplitude of vibration (m)(on Y axis) at station 6 with excitation frequency (Hz)(on X axis)

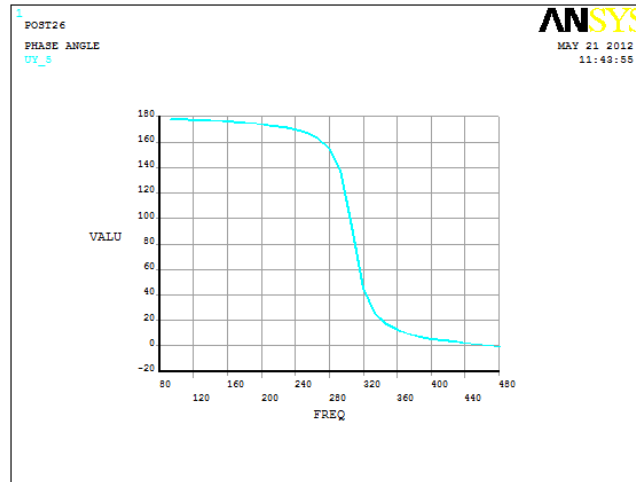


Figure 14: Typical variation of phase angle with excitation frequency

IJSER